PHYSICAL REVIEW C VOLUME 43, NUMBER 4 APRIL 1991

ARTICLES

Coherent photon scattering cross sections for helium near the delta rsonance

D. Delli Carpini, E. C. Booth, and J. P. Miller
Boston University, Boston, Massachusetts 02215

R. Igarashi, J. Bergstrom, H. Caplan, M. Doss, E. Hallin, C. Rangacharyulu, and D. Skopik
Saskatchewan Accelerator Laboratory, Saskatoon, Saskatchewan, Canada S7N 0W0

M. A. Lucas, A. M. Nathan, and D. P. Wells
University of Illinois, 1110 W. Green Street, Urbana, Illinois 61801
(Received 7 November 1990)

The angular distributions for coherent photon scattering from ^{4}He were measured at average laboratory bremsstrahlung energies of 187, 235, and 280 MeV. The experiment was performed at the Saskatchewan Accelerator Laboratory using the new high duty factor electron beam. The scattered photons were observed with a high-resolution NaI(Tl) total absorption scintillation detector. These measurements are intended to investigate modification of the Δ properties inside the nuclear medium and the treatment of nonresonant contributions to the scattering cross sections. The results are compared to theoretical calculations in the isobar-hole model. Clear deviations from the theory are evident at all energies, especially at 187 MeV.

I. INTRODUCTION

The fundamental processes of the photon-nucleon and pion-nucleon interactions at energies near the Δ resonance are dominated by the formation of the Δ isobar. The study of these phenomena in the nucleus is a complex many-body problem. The nuclear medium introduces added degrees of freedom to the system which manifest themselves through modification of the production and decay of the Δ. Different Δ-hole models have been advanced by several authors[1-3] to describe these processes in a unified formalism for pion scattering, pion photoproduction, and photon scattering. Effects such as Fermi motion and multiple pion scattering are partially responsible for these medium modifications. The Fermi motion broadens the resonance by shifting the energy needed to produce the Δ due to the relative motion between the photon and the nucleon. The Δ often decays to a πN channel and the intermediate pion can propagate inside the nuclear medium, undergo multiple scattering, or result in the emission of a real pion. There is an energy shift due to the additional binding of the Δ to the nucleons. The Pauli principle reduces the availability of states into which the Δ can decay (Pauli blocking) leading to a reduction of the Δ resonance width. Another medium effect is the coupling to the pion absorption channel $\Delta N \longrightarrow NN$, a large part of which is expected to be due to the coupling of the Δ to the two-nucleon–two-hole continuum configuration. The pion absorption process is quite complicated, and has been modeled in Koch *et al.*[1] using a spreading potential with variable parameters that have been fitted to the pion scattering data, while Oset and Weise[2] have performed a microscopic calculation of the process.

We present the results of coherent photon scattering differential cross-section measurements from ^{4}He below the peak of the $\Delta(1232)$ resonance. The photon is a useful tool to determine the effect of the nuclear environment on the Δ. One of its advantages is that elastic photon scattering can be used to sample the entire volume of the nucleus since there is almost no attenuation of either the incoming or outgoing photon wave function in the nuclear matter by Coulomb effects or by the strong interaction. This is in contrast to pion elastic scattering and coherent photo-pion production that are dominated by strong interactions near the nuclear surface. Photon scattering provides information that is in several other ways complementary to that given by pion scattering and photoproduction. In photon scattering there is a suppression of coherent forward propagation of photo-produced π^0's in the presence of the ground-state nucleus, while for pions forward π^0 propagation is allowed and is a dominant mechanism in elastic pion scattering. Furthermore, pion scattering can excite only the unnatural parity Δ-hole states, whereas the photon can excite both natural and unnatural parity states.

The Δ-hole theoretical formalism treats the isobar as an elementary specie and focuses on Δ propagation as expressed in the Δ's Green function. Theories[1-3] involving the Δ properties in nuclei assume that the photon excites Δ-hole states which propagate through the nucleus. The models are used to calculate elastic pion-nucleus scatter-

ing, coherent π^0 photoproduction, and coherent photon scattering using a similar theoretical framework for each process.[1,4] The Δ-hole approach includes the influence of the nuclear medium by self-energy or vertex corrections of the Δ-isobar Green function.[1] The formalism makes corrections for complicated many-body Δ-nucleus dynamics by modifying the Δ propagator in the nucleus. All three coherent processes use the same Δ-hole propagator in determining the reaction amplitude. However, the mechanism by which the photon excites the Δ-hole states is very different from that of the pion. The pion coupling to the Δ has a longitudinal vertex function proportional to $\mathbf{s}\cdot\mathbf{k}$, while the photon coupling is transverse and proportional to $\hat{\epsilon}\cdot\mathbf{s}\times\mathbf{k}$, where $\mathbf{k}$ is the γ or π momentum, $\mathbf{s}$ the NΔ transition spin operator, and $\hat{\epsilon}$ is the photon polarization vector. It is this difference in angular dependence in the vertices, for example, which leads to the relative suppression of intermediate π^0's in photon scattering.

A final point concerning photon scattering is that the forward-scattering amplitude can be obtained in principle from data on the total photon absorption cross section in a model-independent way. The imaginary part is obtained from the absorption cross section at energy E using the optical theorem, and the real part is obtained from the Kramers-Kronig dispersion relation, which requires an integration over all energies. No direct measurements of the ^{4}He total photon absorption cross sections in the resonance region exist, but there is a total charged hadron production measurement[5] where the total cross sections are estimated using Monte Carlo corrections for neutral hadron production. Alternatively, there is good experimental evidence that the total photoabsorption cross section per nucleon is about the same for all complex nuclei from Li to Pb in the resonance region.[6] If we extrapolate this to A=4, then we get another estimate of the ^{4}He total absorption cross section, although some caution is necessary since the universality of the cross section fails for deuterium. An estimate of the angular distribution can be obtained by multiplying the forward cross section by the electron scattering form factor squared and by the dipole angular distribution,[7] which gives fair agreement with the curve shapes produced by more sophisticated Δ-hole calculations at forward angles out to perhaps 50°, but generally fails at larger angles.

The experimental measurement of coherent photon scattering is difficult due to the low photon scattering cross sections and the requirement of reasonably good energy resolution. The recent construction of high efficiency detectors with sufficient energy resolution to distinguish the elastic scattered photons from the inelastic scattering and from π^0 decay photons has made coherent photon scattering experiments possible. The advent of high-duty factor electron accelerators permits the measurement of the very small scattering cross sections expected at large angles. Austin *et al.*[8] used the Bates Linear Accelerator bremsstrahlung beam to obtain differential cross-section data for ^{4}He at 180 MeV with a 30 cm × 30 cm NaI detector. The energy resolution of 4.6% was adequate to resolve the coherent scattering from background, since photons that scattered from the first excited state of helium, and the most energetic π^0 photons were both at least 20 MeV below the elastic photon end point. The 180-MeV data overall were in disagreement with the Δ-hole model,[8] especially at the single measured back-angle point at 120°. This discrepancy was thought to be due to an inaccurate calculation of the nonresonant contributions which are small at the resonance, but which are a major component of the cross sections below 200 MeV. For example, dispersion relation calculations[9] of the Compton scattering cross section for the proton show that the nonresonant (Born) contribution is at least 50% of the cross section at 200 MeV but only 15% at the peak of the resonance. It is clear that the nonresonant part of the scattering amplitudes must be handled carefully off resonance.

At higher incident photon energies, the energy difference between elastic photons and decay photons from photoproduced π^0's becomes smaller, and a higher-resolution detector is required. A group working at Bates subsequently used a new high-resolution ($\sim$ 1.7% FWHM for 330 MeV electrons) NaI(Tl) detector (BUNI), developed at Boston University, to measure differential coherent photon scattering cross sections for ^{4}He at an average incident photon energy of 320 MeV, near the peak of the Δ resonance, as reported in Austin *et al.*[10] Forward-angle data were obtained that agreed well with the Δ-hole model calculation of Koch *et al.*[1] We were unable to take data at angles larger than 60° at that time because of the pileup limitation on counting rate due to the low-duty factor of the available photon beam. Since the cross section is expected[1] to be especially sensitive to the details of the Δ - nuclear interaction at angles greater than 60°, the agreement was a necessary but incomplete test of the theory. The database for testing the success of the model with ^{4}He remained small, with only one large angle point (120°) at 180 MeV and no large angle points at 330 MeV. This paper gives experimental results that greatly increase the data base on the low-energy side of the peak of the Δ resonance, where deviations from model predictions have already been noted. Our results show further deviation from the model calculations. Because the SAL accelerator was limited to energies below 300 MeV, we could not pursue these measurements at energies above the peak of the resonance.

II. EXPERIMENTAL APPARATUS AND PROCEDURE

The experiment was performed on the new high-duty factor electron accelerator at the Saskatchewan Accelerator Laboratory (SAL), in Saskatoon, Canada. The facility has a pulse stretcher ring (EROS) to provide a high-duty factor beam of electrons. The duty factor typically varied from 0.3 to 0.6 during the period of the experiment. The beam energy was known absolutely to

±0.2%, and the energy spread of the extracted beam was ±0.1%. A full description of the ring operation and its performance is presented by Dallin.[11]

A diagram of the experimental area is shown in Fig. 1. The bremsstrahlung photon beam was produced by passing the electron beam through a 1% radiation length aluminum foil situated in vacuum just upstream from the electron beam dump magnet. At the bottom of the beam dump hole was a copper beam stop that gave a rough measurement of the beam current from the charge collected. The photons passed through the vacuum tube end window into the air and were collimated by a 1-cm-diameter hole in a 30-cm lead collimator placed in the shield wall. A sweep magnet was used to eliminate secondary electrons from the photon beam. The bremsstrahlung end-point energies used in this experiment were 197, 248, and 291 MeV.

The close proximity of the electron beam dump to the detector and the small volume of the experimental hall made neutron background a major concern. Pileup of low-energy pulses from neutron capture gamma rays limited the data-acquisition rate at large scattering angles, while at small scattering angles the data rate was limited by pileup of low-energy photons produced by the Compton scattering of the bremsstrahlung beam from target electrons. Concrete block shielding was used to reduce the flux of fast neutrons from the beam dump, and a precollimator of 30.5-cm steel was placed between the dump magnet and the collimator to reduce the neutron background from the radiator. A chicane of tanks filled with water was constructed at the access entrance to the hall to reduce the flow of low-energy neutrons into the target room. Most of the remaining neutron background apparently originated in the beam collimator.

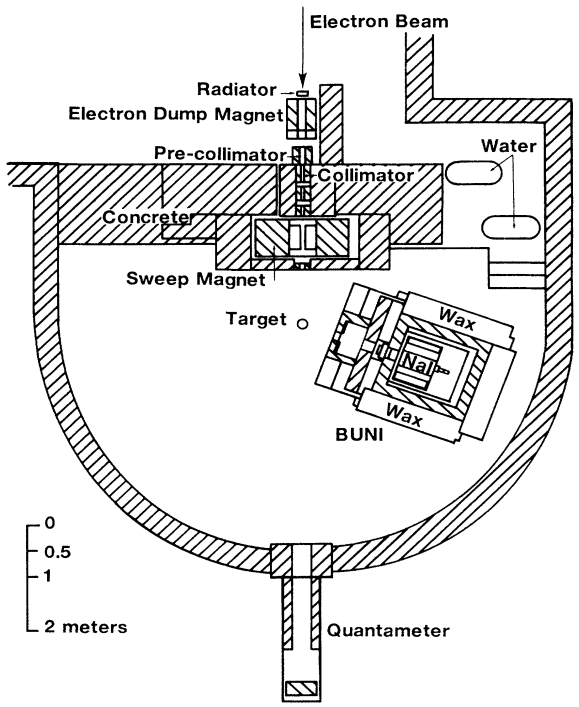

FIG. 1. Schematic diagram of the experimental setup in the EA2 area at SAL.

The NaI crystal was shielded by a box of lead and steel construction, with an equivalent thickness of 19.4 radiation lengths. The box was surrounded by 36 cm of borated paraffin to absorb neutrons. The detector with its shielding rested on a steel table which could be raised and leveled by motorized jacks. Air pads were used to move the 20-tonne apparatus to the various scattering angles. Additional lead shielding was constructed in front of the detector collimator to further reduce the low-energy room background.

The detector used was a high-resolution NaI(Tl) total absorption scintillation counter (BUNI) designed at Boston University. It is segmented into five optically isolated cylindrical sections. The core has a diameter of 26.7 cm and a length of 55.9 cm. The annular part is 10.8 cm thick. The core segment and each quadrant are all optically isolated. The NaI sections are surrounded by a 12.7-cm-thick BC 400 plastic-scintillator annulus used to reject cosmic rays. Further details of the detector design and performance can be found in Miller *et al.*[12] To improve cosmic-ray rejection the front and rear ends of the detector were covered with six additional plastic scintillators, 2.54 cm thick. The scattered photons entered the crystal through a 12.5-cm-diameter tungsten collimator. A 22.9-cm-long cylinder of beryllium was inserted in front of the aperture to reduce low-energy photons from the scattered beam and room background. One thin veto scintillator in addition to the cosmic-ray veto was placed between the beryllium and the tungsten collimator, and two other scintillators were placed in front of the beryllium hardener to reject high-energy electrons entering the detector.

The liquid-^{4}He target was mounted in a target ladder framework on top of a steel post which was bolted to the floor. The target holder had four vertical positions that could be changed remotely; these corresponded to the full helium target, the dummy empty helium target, a carbon target, and no target. Other details of the target construction can be found in Wells.[13] A laser mounted on a goniometer was built into the base of the pivot post, so that the scattering angle could be measured to a fraction of a degree. Because of the limited room space, the target position was moved down the beam line when large-angle data was taken. Further details about the experimental setup can be found in Delli Carpini.[14]

III. DATA REDUCTION

There are 19 photomultiplier tubes viewing the NaI detector. Signals from all 19 tubes were summed off line to provide a total signal proportional to the energy of the scattered photon. The scattered photon was an "event" if it triggered a discriminator fed by a hard wired sum of the seven core tubes, with the discriminator set well

above room background, typically at half the accelerator energy. To perform the summation properly in software it was necessary to measure the gain of each phototube and to monitor any changes in gain during data acquisition. The gains of the photomultiplier signals varied slightly over time due to temperature changes, high data rates, or high voltage drift. The phototube gains were calibrated using direct bremsstrahlung into the NaI core, and pulses from a xenon light flasher were used to follow drifts in the gain. The light from the xenon flasher was fanned out via fiber-optic cables to each NaI element in the crystal. The ADC channel position of the flasher peak in the data spectra was set above the data to avoid accidental contamination. In order to correct for possible drifts in the xenon light source, a 5.1-cm NaI crystal was used to monitor the 2.615-MeV gamma ray from a thorium source along with the xenon flasher pulse. Relative changes of the flasher peaks in all the phototubes were then compared to changes of the 5.1-cm NaI flasher peak with respect to the thorium peak channel to obtain corrected photomultiplier gains for each run. In this experiment the gain shifts were tracked to within 0.5%.

No event above the NaI threshold was rejected on line using hardware vetos from plastic-scintillator counters, but every event was recorded to tape in order to make the decision in software. The gain of the core NaI section was obtained at every change in beam energy by moving BUNI on its platform to zero degrees and putting a low intensity bremsstrahlung beam into it. The beam was attenuated by placing 10 cm of lead in front of the beam collimator, reducing the beam intensity by a factor of 10^4. A spectrum with no pulse pileup was obtained using a 1 nA electron beam current. Periodically throughout the data runs a thorium source was placed in the BUNI collimator to calibrate the four outer sections of the NaI annulus surrounding the core. A low-energy gamma ray was effective for this purpose since only 5–10 MeV of the total gamma ray energy typically was deposited in a quadrant. Gains were computed and assigned for the separate data runs at each detector angle, and the entire set of runs were summed off line to obtain the proper scattered photon spectrum. Core gains were revised once for each run and typically 5 runs of 1-2 h each were summed to constitute the data at one angle. It was unnecessary to revise the quadrant section gains from run to run since their contribution to the total energy spectra was small and the change in the quadrant calibration was less than 0.5% from day to day. Once the total energy spectrum was obtained, background such as data triggered by cosmic rays, photons radiated from electron pairs produced in the beryllium absorber, and charged particles produced in the target was eliminated in software. Cosmic rays were the dominant full energy background and had to be rejected with high effiiciency. If a signal in any of the cosmic-ray veto plastic scintillators was above a determined threshold, the event was rejected. The threshold values were adjusted in software to eliminate a large fraction of the cosmic rays but only a small fraction of actual data. The elimination of cosmic rays by the plastic shield alone was at the 99.0% level. To improve the cosmic-ray rejection another cut was made that used the ratio between the total energy deposited in the NaI annulus and the total energy deposited in the detector. By rejecting any event with a ratio above 0.2 the cosmic-ray rejection was brought to 99.9%. This reduced the cosmic-ray rate in the 290-MeV region to 0.14 count/MeV h and in the 200-MeV region to about 0.04 count/MeV h. This high rejection factor was needed for measuring very small Compton scattering cross sections of a few nb/sr.

An important possible source of data distortion was pileup due to the simultaneous acquisition of a high-energy photon with a low-energy background photon. This effect could shift π^0 photons into the Compton scattering energy region or move Compton scattered photons above the kinematic end point. The fraction of pileup events was determined from the pedestal event histograms obtained by accepting events triggered at a random low rate . The effect of pileup was most noticeable in the NaI core, which could "see" room and target background through the open collimator. The pileup rate was periodically monitored and the electron beam current adjusted to maintain an average total pileup rate of under 3% for pulses with energy of more than 2 MeV, which was adequate to provide data with negligible distortion. This percentage was determined by summing the number of counts above 2 MeV and dividing by the total number of counts. The accelerator beam intensity of 1–2 μA at large detector angles had to be reduced to 0.2 μA with the detector at far forward angles in order to keep the pileup at acceptable levels.

The NaI detector response function for monoenergetic photons has a fairly sharp upper limit but a long low-energy tail due to shower leakage.[12] In summing up the Compton scattered events in a 10- or 15-MeV photon energy interval, one must know the detector efficiency, that is, what fraction of events were lost in the tail. The detector response was obtained using the EGS computer code.[15] The code used the experimental geometry including the collimators, beryllium absorber, and veto scintillators, and the program followed the incident photon until all of its energy was deposited in the materials it penetrated. EGS calculations were performed for monochromatic photons at 10-MeV intervals to cover the range of the bremsstrahlung photon beam used in the experiment. The response functions then were used by another Monte Carlo program to simulate the response to bremsstrahlung elastic scattered photons and π^0 decay photons, assuming no angular or energy dependence for the scattering. The incident photon on the target was randomly selected from the bremsstrahlung spectrum and allowed to scatter or produce a π^0 in a random direction. If the elastic photon or π^0 decay photons are within the detector solid angle, they are distributed according to the response function for that particular energy. Alternatively, the photons entering the solid angle can be accumulated without the effect of the detector re-

sponse function included. The ratio of these two numbers in an energy interval is the *efficiency* of the detector. This ratio is used to obtain the number of elastically scattered photons from the measured photon spectra.

The simulated π^0 decay photon spectra and elastic scattered photon spectra are fitted to the data with scaling factors for each process. The fitted data also served to give an additional check on the energy calibration. An example of the scattered photon spectrum at 30° for 291 MeV electrons with the computer simulation fit to the background-subtracted data is shown in Fig. 2. The spectrum was produced by summing together all the runs taken at 30° using the appropriate relative gains while rejecting events due to background. The fit is good, which shows the gain-shifting procedure and the computer simulations are adequate. The target-empty runs were made with a dummy target identical to the ^{4}He target. The target-empty spectrum also is shown in Fig. 2. All of the other data showed similar fits. The bremsstrahlung shape with the appropriate attenuation due to any absorber placed in the beam line can also be simulated with EGS. The shape for a 10-cm lead absorber fitted to the zero-degree calibration data spectra is shown in Fig. 3. The end point in the spectrum corresponds to the full beam energy. The bremsstrahlung shape used is that obtained by Mathews and Owens,[16] folded with the detector response function. The good fit gives confidence in the EGS simulation, which was already known to be reliable.[12] The energy resolution of the detector was checked at SAL by measuring the elastic electron scattering from ^{12}C and ^{27}Al targets. The measured resolution of 2% FWHM was in agreement with EGS simulations which included the broadening effects of the plastic scintillator vetos on the electron peak.

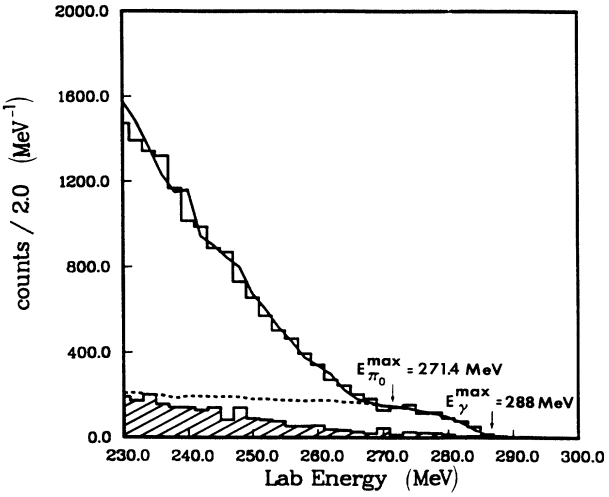

FIG. 2. Elastic scattered photon spectrum off ^{4}He at 30° and 291 MeV incident photon end point energy. The solid line is a computer-simulated spectrum fitted to the data. The shaded area is the target-empty spectrum. The dashed line is the elastic scattered photon contribution to the total spectrum.

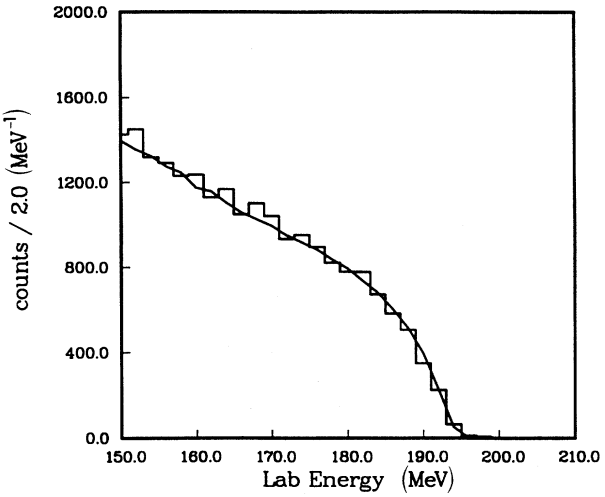

FIG. 3. Direct bremsstrahlung data with computer-simulation fit.

The number of photons incident on the target is determined from the total charge acquired on a quantameter during the run. The Wilson quantameter[17] is designed to produce a measured ionization charge proportional to the total energy delivered by the beam. The measured quantameter charges were corrected due to absorption in the materials in front of the quantameter. The proportionality constant characterizes the particular quantameter and is independent of the spectral shape of the bremsstrahlung beam or whether the beam is made of electrons or photons. The quantameter used was $QB1$, originally from the Cambridge Electron Accelerator. It was calibrated with the electron beam at Bates and cross calibrated against a standard NBS P2 chamber[18] at SAL.

The differential cross section was calculated from

$$\frac{d\sigma}{d\Omega}(\theta, E_{\rm av}) = \alpha \frac{C_{\rm net}(E_1', E_2')}{\Delta\Omega\, N_\gamma(E_1, E_2)\, N_T\, \epsilon(E_1', E_2')}\ , \qquad (1)$$

where $C_{\rm net}(E_1', E_2')$ is the net number of counts in the elastically scattered photon spectrum between energies E_1' and E_2' in a solid angle $\Delta\Omega$, $N_\gamma(E_1, E_2)$ is the number of incident photons on the target between energies E_1 and E_2, N_T is the number of target nuclei per unit area, α is the correction factor due to absorption in the materials between the target and the detector, and $\epsilon(E_1', E_2')$ is the efficiency of the detector. The energies E_1 and E_2 are incident energies in the laboratory frame and the energies E_1' and E_2' are the corresponding scattered energies with the kinematic shift for the target recoil. The energy $E_{\rm av}$ is the average incident photon energy, for the interval used to calculate the differential cross section, weighted by the number of photons per unit energy interval. The interval used to determine the net counts is typically 2 MeV above the maximum π^0 decay photon end point and 5 MeV below the elastic scattered photon end point. The elimination of the top 5 MeV of the spectrum reduces the

effect of the energy calibration error and the uncertainty in the theoretical number of photons in the top few MeV. The absorption correction factor alpha was calculated by an EGS simulation to be 1.83, which included four plastic scintillators with a total thickness of 3.28 gm/cm^2 and the beryllium hardener with a thickness of 40.9 gm/cm^2. The absorption correction due to the helium target was calculated to be 1.038.

IV. RESULTS AND CONCLUSION

Angular distributions for the coherent photon scattering from ^{4}He were measured at average incident bremsstrahlung photon laboratory energies of 187, 235, and 280 MeV. The angular distributions are shown in Figs. 4–6. Numerical values of the cross sections and estimated error are given by Delli Carpini.[14] Δ-hole model calculations[1] for the 187-MeV and 280-MeV data are shown for comparison. The dashed curve in each figure is the result obtained by using the simple model[7] $d\sigma(E,\theta)/d\Omega = \frac{1}{2}(1+\cos^2\theta)|\,F(q)\,|^2 d\sigma(E,0)/d\Omega$, where $F(q)$ is the electron scattering form factor and $d\sigma(E,0)/d\Omega$ is the forward-scattering cross section found from using total photoabsorption cross-section data, the optical theorem and the dispersion relation. The forward-angle cross sections at 235 MeV (1.8 ± 0.3 μb/sr) and 280 MeV (3.8 ± 0.5 μb/sr) were obtained using the Bonn total absorption data,[5] and the resulting dashed curves (Figs. 5 and 6) are in fairly good agreement with our data. The 187-MeV (0.29 ± 0.10 μb/sr) point was obtained using the average total absorption cross section per nucleon in many nuclei from Ahrens *et al.*,[6] since there is no Bonn data at this energy, but the agreement with our data is not very good (Fig. 4). The Ahrens *et al.*[6] absorption cross sections are not in good agreement with the Bonn data for ^{4}He, having the peak cross section at a higher energy than that found at Bonn. Also one can see that the 187-MeV data are in poor agreement with the Δ-hole calculation, especially at back angles where the data show a substantial rise in the cross section. This was already seen from previous data taken by Austin *et al.*[8] at an average bremsstrahlung energy of 180 MeV, but the present data with many more data points confirm the increase in cross section at the back angles. The 280-MeV data also do not agree very well with the Δ-hole theoretical prediction shown by the solid line, but the overall shape of the theoretical spectrum follows the data much better than at 187 MeV.

A comparison of the 320-MeV Bates data[10] with our

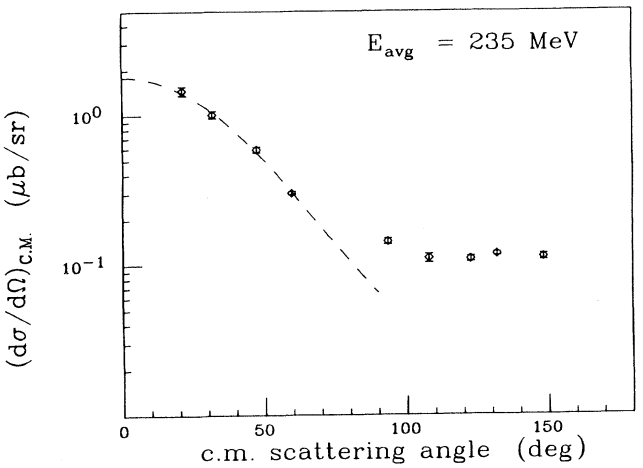

FIG. 5. Elastic photon differential cross section at an average laboratory energy of 235 MeV. The error bars are statistical. The dashed line is the schematic model curve using $d\sigma(E,\theta=0)/d\Omega = 1.8\pm0.3$ μb/sr.

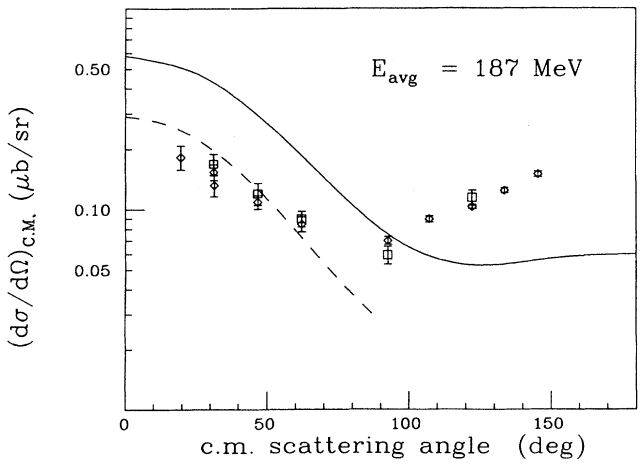

FIG. 4. Elastic photon differential cross section (◇) at an average laboratory energy of 187 MeV. The (□) data points are at an average laboratory energy of 180 MeV taken from Ref. 8. The error bars are statistical. The solid line is the Δ-hole calculation.[1] The dashed line is the schematic model curve using $d\sigma(E,\theta=0)/d\Omega = 0.29\pm0.10$ μb/sr.

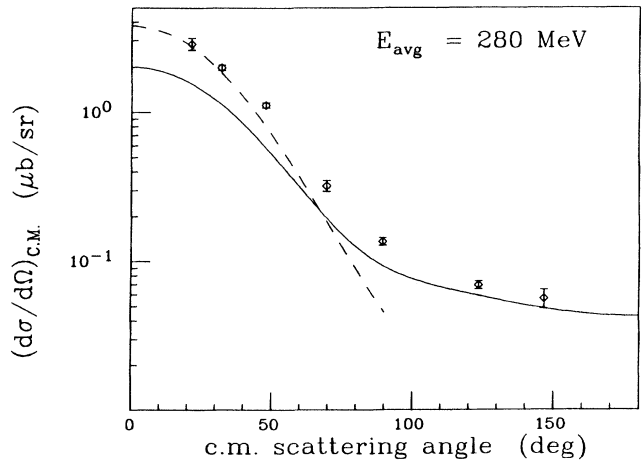

FIG. 6. Elastic photon differential cross section at an average laboratory energy of 280 MeV. The error bars are statistical. The solid line is the Δ-hole calculation.[1] The dashed line is the schematic model curve using $d\sigma(E,\theta=0)/d\Omega = 3.8\pm0.5$ μb/sr.

280-MeV data shows that the small-angle cross sections at 280 MeV are about the same as at 320 MeV. This agrees approximately with the peak in the Bonn photo absorption data, but is 20-30 MeV lower than the peak position predicted in Koch *et al.*,[1] who discuss this problem. There are no available adjustable parameters, so that agreement with the data cannot be forced without substantial revisons to the model.

This experiment greatly increases the experimental data base for the reaction ^{4}He$(\gamma,\gamma)^4$He in the energy region below the the Δ resonance peak and the results do not agree with the Δ-hole calculations. The shape of the calculated differential cross sections do not fit the data at low energy and the calculated forward-angle cross sections also are not in good agreement with the data. These results indicate that the recent Δ-hole model description of coherent photon scattering, π^0 production, and pion scattering is not successful for ^{4}He below the peak of the nucleon Δ resonance. As previously noted, the nonresonant contributions to coherent scattering will be large at low energy and may not have been correctly included in the model. A significant test of the unified approach of the Δ-hole model using Compton scattering cannot be made until the model is corrected to properly include the nonresonance background contributions. Compton scattering measurements should be able to determine, for example, whether the spreading potential obtained from pion scattering at the nuclear surface can be used to describe photon scattering from deep inside the nucleus. Additional coherent scattering measurements at higher energies through and above the peak of the nucleon resonance are needed to trace out possible further deviations from model predictions. It should also be noted that the database for the complementary reaction of π^0 photoproduction from ^{4}He and other nuclei is extremely small, with only one measurement of coherent photoproduction, taken near the peak of the resonance.[19] Experimental results of Compton scattering from ^{1}H and ^{12}C at SAL are available and are being analyzed. They may help to determine if the fundamental scattering from the nucleon is well represented by the model, and to learn if the model does a better job of describing scattering from a nucleus with more nucleons and a larger volume.

ACKNOWLEDGMENTS

We are pleased to acknowledge the great efforts made by the entire SAL staff which made it possible to carry out this experiment in an early period of running the new stretcher ring. This work was supported by the National Science Foundation and the Natural Sciences and Engineering Research Council of Canada.

[1] J. H. Koch, E. J. Moniz, and N. Ohtsuka, Ann. Phys. (N.Y.) **54**, 99 (1984).
[2] E. Oset and W. Weise, Nucl. Phys. **A368**, 375 (1981); *ibid.* **A329**, 402 (1979).
[3] W. Weise, Nucl. Phys. **A358**, 163 (1981).
[4] J. H. Koch and N Ohtsuka, Nucl. Phys. **A435**, 765 (1985).
[5] H. Rost, Bonn Report IR-80-10, 1980.
[6] J. Ahrens, Nucl. Phys. **A446**, 229 (1985); J. Ahrens, L. S. Ferreira, and W. Weise, Nucl. Phys. **A485**, 621 (1988).
[7] E. Hayward and B. Ziegler, Nucl. Phys. **A414**, 333 (1984).
[8] E. J. Austin, E. C. Booth, E. K. McIntyre, J. P. Miller, B. L. Roberts, D. A. Whitehouse, and G. Dodson, Phys. Rev. Lett. **57**, 972 (1986).
[9] W. Pfeil, H. Rollnik, and S. Stankowski, Nucl. Phys. **B73**, 166 (1974).
[10] E. J. Austin, E. C. Booth, D. Delli Carpini, K. P. Gall, E. K. McIntyre, J. P. Miller, D. Warner, D. A. Whitehouse, and G. Dodson, Phys. Rev. Lett. **61**, 1922 (1988).
[11] L. O. Dallin, IEEE Particle Accelerator Conference (1989) p. 22.
[12] J. P. Miller, E. J. Austin, E. C. Booth, K. P. Gall, E. K. McIntyre, and D. Whitehouse, Nucl. Instrum. Methods Phys. Res., **A270**, 431 (1988).
[13] D. P. Wells, Ph.D. dissertation, University of Illinois, Urbana, 1990.
[14] D. Delli Carpini, Ph.D. dissertation, Boston University, 1990.
[15] W. R. Nelson, H. Hirayama, and D. W. O. Rogers, EGS4 Code System, SLAC-265, 1985.
[16] J. L. Mathews and R. O. Owens, Nucl. Instrum. Methods, **111**, 157 (1973).
[17] R. R. Wilson, Nucl. Instrum. **1**, 101 (1957).
[18] J. S. Pruitt and S. R. Domen, N.B.S. monograph **48** (1962).
[19] D. R. Tieger, E. C. Booth, J. P. Miller, B. L. Roberts, J. Comuzzi, G. W. Dodson, S. Gilad, and R. P. Redwine, Phys. Rev. Lett. **53**, 755 (1984).